

# Manifestation of the Hofstadter butterfly in far-infrared absorption

Vidar Gudmundsson

*Science Institute, University of Iceland, Dunhaga 3, IS-107 Reykjavik, Iceland.*

Rolf R. Gerhardt

*Max-Planck-Institut für Festkörperforschung, Heisenbergstraße 1, D-70569 Stuttgart,  
Federal Republic of Germany*

(October 5, 2018)

## Abstract

The far-infrared absorption of a two-dimensional electron gas with a square-lattice modulation in a perpendicular constant magnetic field is calculated self-consistently within the Hartree approximation. For strong modulation and short period we obtain intra- and intersubband magnetoplasmon modes reflecting the subbands of the Hofstadter butterfly in two or more Landau bands. The character of the absorption and the correlation of the peaks to the number of flux quanta through each unit cell of the periodic potential depends strongly on the location of the chemical potential with respect to the subbands, or what is the same, on the density of electrons in the system.

71.20.-b 73.20.Dx 73.20.Mf 78.66.Fd

Indications of the Hofstadter subband structure [1,2] of the Landau bands of a two-dimensional electron gas (2DEG) in square modulated lateral superlattices have been believed to be found directly [3] and indirectly [4] in transport measurements. This opens the important question of whether the subband structure can directly be detected in far-infrared (FIR) absorption measurements. Calculations of the ground state properties of the laterally modulated 2DEG indicate that the strong screening effects would hamper an observation of even the coarse structure of the Hofstadter butterfly in, e.g. magnetocapacitance or magnetoresistance measurements, unless very short periods and strong modulation would be used [5]. But what about FIR measurements?

The FIR-absorption is determined by the self-consistent field which describes the dynamical screening of the incident external field. Since, as calculations [5] show, screening is also very important in the ground state, screening effects should be treated on equal footing in both the ground state and in the FIR response. That an inconsistent treatment of screening effects may lead to qualitatively wrong results in a 2DEG with strong lateral modulation is known from the case of quantum dots. There, according to the generalized Kohn's theorem [6,7], Coulomb interaction effects on the ground state and dynamical response of a parabolically confined electron system cancel, so that the dot responds at the bare single-electron frequencies. This experimentally confirmed fact has been reproduced only by those many-body calculations which have treated the interaction effects in the ground state and in the FIR response on the same footing. Results of such calculations have been published for isolated quantum dots [8,9] and for unidirectionally modulated 2DEG [10,11], but to our knowledge no corresponding results are available for the square modulation.<sup>1</sup>

The square lateral superlattice with period  $L$  is spanned by the lattice vectors  $\mathbf{R} = m\mathbf{l}_1 + n\mathbf{l}_2$ , where  $\mathbf{l}_1 = L\hat{\mathbf{x}}$ , and  $\mathbf{l}_2 = L\hat{\mathbf{y}}$  are the primitive translations of the Bravais lattice  $\mathcal{B}$ ;  $n, m \in \mathbb{Z}$ . The reciprocal lattice  $\mathcal{R}$  is spanned by  $\mathbf{G} = G_1\mathbf{g}_1 + G_2\mathbf{g}_2$ , with  $\mathbf{g}_1 = 2\pi\hat{\mathbf{y}}/l_1$ ,  $\mathbf{g}_2 = 2\pi\hat{\mathbf{x}}/l_2$ , and  $G_1, G_2 \in \mathbb{Z}$ . The ground-state properties of the interacting 2DEG in a perpendicular homogeneous magnetic field  $\mathbf{B} = B\hat{\mathbf{z}}$  and the periodic potential  $V(\mathbf{r}) = V_0\{\cos(g_1x) + \cos(g_2y)\}$  are calculated in the Hartree approximation. The Hartree single electron states  $|\alpha\rangle$  and their energies  $\varepsilon_\alpha$  are labelled by the quantum numbers  $\{n_l, \mu, \nu\} = \alpha$ , where  $n_l \geq 0$  is a Landau band index,  $\mu = (\theta_1 + 2\pi n_1)/p$ ,  $\nu = (\theta_2 + 2\pi n_2)/q$ , with  $n_1 \in I_1 = \{0, \dots, p-1\}$ ,  $n_2 \in I_2 = \{0, \dots, q-1\}$ ,  $\theta_i \in [-\pi, \pi]$ , and  $pq \in \mathbb{N}$  is the number of magnetic flux quanta through the lattice unit cell. The Hartree states are expanded in terms of the symmetric basis functions constructed by Ferrari [12] and used by Silberbauer [13] and the present authors [5]. The Ferrari basis is complete provided that  $(\mu, \nu) \neq (\pi, \pi)$  for all  $(n_1, n_2) \in I_1 \times I_2$ . The Hartree potential “felt” by each electron and caused by the total electronic charge density of the 2DEG,  $-en_s(\mathbf{r})$ , and the positive neutralizing background charge,  $+en_b$ , together with the external periodic potential  $V(\mathbf{r})$  do not couple states at different points in the quasi-Brillouin zone  $\theta = (\theta_1, \theta_2) \in \{[-\pi, \pi] \times [-\pi, \pi]\}$ . However, states at a given point depend, in a self-consistent way, on states in the whole zone through  $n_s(\mathbf{r})$  [13,5]. The periodic potential broadens the Landau levels into Landau bands that

---

<sup>1</sup>The collective excitations of a 2DEG with a two-dimensional magnetic-field modulation have been studied by X. Wu and S. E. Ulloa in Phys. Rev. B **47**, 10028 (1993), but without considering interaction effects in the ground state.

due to the comensurability conditions between  $L$  and the magnetic length  $l = (c\hbar/eB)^{1/2}$ , are split into  $pq$  subbands. The resulting energy spectrum, the Hofstadter butterfly [1,2], retains essentially its complicated gap structure but is strongly reduced in symmetry by the electron-electron interaction [5] and coupling to higher Landau bands caused by the periodic potential [14]. The symmetry depends on the mean electron density, or, equivalently, the chemical potential.

In order to calculate the FIR absorption of the 2DEG we perturb this by a monochromatic external electric field:

$$\mathbf{E}_{ext}(\mathbf{r}, t) = -i\mathcal{E}_0 \frac{\mathbf{k} + \mathbf{G}}{|\mathbf{k} + \mathbf{G}|} \exp \{i(\mathbf{k} + \mathbf{G}) \cdot \mathbf{r} - i\omega t\}. \quad (1)$$

Here we do not restrict the dispersion relation for the external field,  $\omega(\mathbf{k} + \mathbf{G})$ , to that of a free propagating electromagnetic wave, instead we allow for the more general situation in which the external field is produced as in a near-field spectroscopy or in a Raman scattering set-up. The power absorption is found from the Joule heating of the self-consistent electric field [15,8],  $-\nabla\phi_{sc}$ , with  $\phi_{sc} = \phi_{ext} + \phi_{ind}$ ,

$$P(\mathbf{k} + \mathbf{G}, \omega) = -\frac{\omega}{4\pi} [|\mathbf{k} + \mathbf{G}| \phi_{sc}(\mathbf{k} + \mathbf{G}, \omega) \phi_{ext}^*(\mathbf{k} + \mathbf{G}, \omega)]. \quad (2)$$

The induced potential  $\phi_{ind}$  is caused by the density variation  $\delta n_s(\mathbf{r})$  due to  $\phi_{sc}$ , which can then in turn be related to the external field by the dielectric matrix

$$\sum_{\mathbf{G}'} \epsilon_{\mathbf{G}, \mathbf{G}'}(\mathbf{k}, \omega) \phi_{sc}(\mathbf{k} + \mathbf{G}', \omega) = \phi_{ext}(\mathbf{k} + \mathbf{G}, \omega). \quad (3)$$

The dielectric tensor,  $\epsilon_{\mathbf{G}, \mathbf{G}'}(\mathbf{k}, \omega) = \delta_{\mathbf{G}, \mathbf{G}'} - \frac{2\pi e^2}{\kappa|\mathbf{k} + \mathbf{G}|} \chi_{\mathbf{G}, \mathbf{G}'}(\mathbf{k}, \omega)$ , is determined by the susceptibility of the 2DEG

$$\chi_{\mathbf{G}, \mathbf{G}'}(\mathbf{k}, \omega) = \frac{1}{(2\pi L)^2} \int d\theta \sum_{\alpha, \alpha'} f_{\alpha, \alpha'}^{\theta, \theta - \mathbf{k}L}(\hbar\omega) \frac{J_{\alpha, \alpha'}^{\theta, \theta - \mathbf{k}L - \mathbf{G}L}(\mathbf{k} + \mathbf{G})}{\left( J_{\alpha, \alpha'}^{\theta, \theta - \mathbf{k}L - \mathbf{G}L}(\mathbf{k} + \mathbf{G}') \right)^*}, \quad (4)$$

where  $\mathbf{k}$  is in the first Brillouin zone,  $\kappa$  is the dielectric constant of the surrounding medium,

$$f_{\alpha, \alpha'}^{\theta, \theta'}(\hbar\omega) = \left\{ \frac{f^0(\varepsilon_{\alpha, \theta}) - f^0(\varepsilon_{\alpha', \theta'})}{\hbar\omega + (\varepsilon_{\alpha, \theta} - \varepsilon_{\alpha', \theta'}) + i\hbar\eta} \right\} \quad (5)$$

in which  $f^0$  is the equilibrium Fermi distribution,  $\eta \rightarrow 0^+$ , and

$$J_{\alpha, \alpha'}^{\theta, \theta'}(\mathbf{k}) = (\alpha'(\theta') | e^{-i\mathbf{k} \cdot \mathbf{r}} | \alpha(\theta)). \quad (6)$$

Special care must be taken with respect to the symmetry of the wave functions corresponding to the Hartree states  $|\alpha(\theta)\rangle$  when translating them across the boundaries of the quasi-Brillouin zones. The peaks in the absorption spectra represent absorption of collective modes of the 2DEG. Single-electron transitions and collective oscillations can be identified as zeros of the real part of the determinant of the dielectric matrix. For the collective oscillations the imaginary part simultaneously vanishes but becomes very large for the single electron transitions indicating the strong damping of such processes. Here we prefer to

calculate  $P(\mathbf{k} + \mathbf{G}, \omega)$  for a monochromatic external field instead of searching for zeros of  $\det\{\epsilon_{\mathbf{G}, \mathbf{G}'}\}$  in order to avoid the complication of multiple branches of the magnetoplasmon dispersion for different reciprocal lattice vectors  $\mathbf{G}$ . The response of the system can also be analyzed in more detail by imposing a certain symmetry or polarization on the external field. Although we study collective oscillations here, it is still possible to identify in many cases the most important single-electron transitions contributing to the collective mode, either from the dispersion or by restricting the type of single electron transitions in the calculation.

In the numerical calculations we use GaAs parameters,  $m^* = 0.067m_0$ , and  $\kappa = 12.4$ . The power dissipation of the 2DEG is made possible by retaining a small but finite imaginary part for the frequency in the susceptibility, Eqs. (4) and (5). We choose  $\eta = \omega_c/50$ . In order to examine the fine structure of the magnetoplasmon dispersion we have chosen a monochromatic external perturbing field (1) with  $\mathbf{G} = 0$  and  $\mathbf{k}$  in the first Brillouin zone.

The absorption of a homogeneous 2DEG ( $V_0 = 0$ ) is compared in Fig. 1 with the first-order dispersion in  $\mathbf{k}$  of a magnetoplasmon,  $\omega^2 = \omega_c^2 + 2\pi e^2 n_s k / (\kappa m^*)$ . Kohn's theorem manifests itself by the fact that only one peak is visible for  $\mathbf{k} \rightarrow 0$  [7], and for finite wave vectors  $\mathbf{k}$  the magnetoplasmon interacts with harmonics of the cyclotron resonance, resulting in so the called Bernstein modes [16–18].

To make the Hofstadter subband structure of the Landau bands discernible, we have to resort to short periods  $L = 50$  nm and strong modulation  $V_0 = 4$  meV, just as we had to in order to observe the subbands in the thermodynamic density of states [5]. In addition, the structures are very sensitive to the location of the chemical potential with respect to the subbands, i.e. to the filling factor  $\nu$  of the Landau bands. Figure 2a shows the absorption for  $\nu = 1/2$ , and the low frequency part is reproduced in Fig. 2b. In Fig. 2c the subband dispersion in one quasi-Brillouin zone along several values of  $\theta_2$  is projected onto the  $\theta_1$ -axis, thus indicating the bandwidths and the position of the chemical potential. Since one and a half subband in the lowest Landau band are filled, and it is not inhibited by a selection rule, we can see *three intraband* magnetoplasmons. The  $k$ -dispersion allows the following identification in Fig. 2b: The lowest frequency peak is the plasmon with contributions from transitions between the upper two subbands, the center peak gets contributions from the two lowest subbands and the high frequency peak has contributions connecting the lowest and the top subband. Since only two subbands of the lowest Landau band are occupied (of which one is partially filled), only two peaks are found for the *interband* magnetoplasmon with frequency just above  $\omega_c$ . The absorption for the same situation but for a different filling factor, i.e.  $\nu = 5/6$ , is seen in Fig. 3. Now all the three subbands of the lowest Landau band are at least partially occupied and *three interband* magnetoplasmon absorption peaks are clearly discernible. For  $\nu = 1$  the low frequency intraband peaks vanish and the interband peak with the lowest frequency accounts for almost all of the oscillator strength. The structure of the Hofstadter spectrum can be seen for other values of  $pq$  in the calculations. In Fig. 4 the absorption for the cases  $pq = 2$  and  $pq = 4$  is seen for quite different parameters. The double structure expected for  $pq = 2$  is visible for relatively large period,  $L = 100$  nm, and weak modulation  $V_0 = 0.4$  meV, while two of the four peaks for the case of  $pq = 4$  are just appearing for  $V_0 = 3$  meV, and  $L = 50$  nm. This reflects the stronger screening of the 2DEG observed in the ground state calculations [5] for higher values of  $pq$ , where a strong modulation and short period were needed to see structure in the thermodynamic density of states caused by the Hofstadter subbands. In addition, here the filling factor  $\nu$  not only

determines the strength of the screening and thus the relevance of selection rules, but it is also essential to control in order to occupy subbands such that single electron transitions can take place contributing to the collective oscillations.

It is interesting to note that in the case of a nonvanishing potential modulation,  $V_0 \neq 0$ , the absorption  $P(\omega)$  has a nontrivial structure, even for the case  $\mathbf{k} \rightarrow 0$ . The condition for the validity of the generalized Kohn's theorem can thus be violated by either spatially modulating the time-dependent external electric field (1) or by the static potential  $V(\mathbf{r})$  the 2DEG resides in.

In summary, the FIR-absorption of a 2DEG in a short-period strongly modulated square lateral superlattice shows the underlying Hofstadter subband structure. The structure can be seen in the absorption due to either intra- or interband magnetoplasmons by tuning the density or the filling factor within the lowest Landau band. The intraband magnetoplasmon peaks in the absorption have weak oscillator strengths compared to the interband absorption and are situated in a region on the energy scale that is difficult to detect with present day FIR technology.

## ACKNOWLEDGMENTS

We thank Dr. B. Farid for an interesting discussion. This research was supported in part by the Icelandic Natural Science Foundation, the University of Iceland Research Fund, and a and a NATO collaborative research Grant No. CRG 921204.

## REFERENCES

- [1] R. D. Hofstadter, Phys. Rev. B **14**, 2239 (1976).
- [2] D. Pfannkuche and R. Gerhardts, Phys. Rev. B **46**, 12606 (1992).
- [3] T. Schloesser, K. Ensslin, J. P. Kotthaus, and M. Holland, Europhys. Lett. **33**, 683 (1996).
- [4] R. R. Gerhardts, D. Weiss, and U. Wulf, Phys. Rev. B **43**, 5192 (1991).
- [5] V. Gudmundsson and R. R. Gerhardts, Phys. Rev. B **52**, 16744 (1995).
- [6] P. A. Maksym and T. Chakraborty, Phys. Rev. Lett **65**, 108 (1990).
- [7] W. Kohn, Phys. Rev. **123**, 1242 (1961).
- [8] V. Gudmundsson and R. Gerhardts, Phys. Rev. B **43**, 12098 (1991).
- [9] D. Pfannkuche and R. Gerhardts, Phys. Rev. B **44**, 13132 (1991).
- [10] U. Wulf *et al.*, Phys. Rev. B **41**, 3113 (1990).
- [11] U. Wulf *et al.*, Phys. Rev. B **42**, 7637 (1990).
- [12] R. Ferrari, Phys. Rev. B **42**, 4598 (1990).
- [13] H. Silberbauer, J. Phys. C **4**, 7355 (1992).
- [14] G. Petschel and T. Geisel, Phys. Rev. Lett. **71**, 239 (1993).
- [15] C. Dahl, Phys. Rev. B **41**, 5763 (1990).
- [16] I. B. Bernstein, Phys. Rev. **109**, 10 (1958).
- [17] N. J. M. Horing and M. M. Yildiz, Ann. Phys. **97**, 216 (1976).
- [18] E. Batke, D. Heitmann, and C. W. Tu, Phys. Rev. B **34**, 6951 (1986).

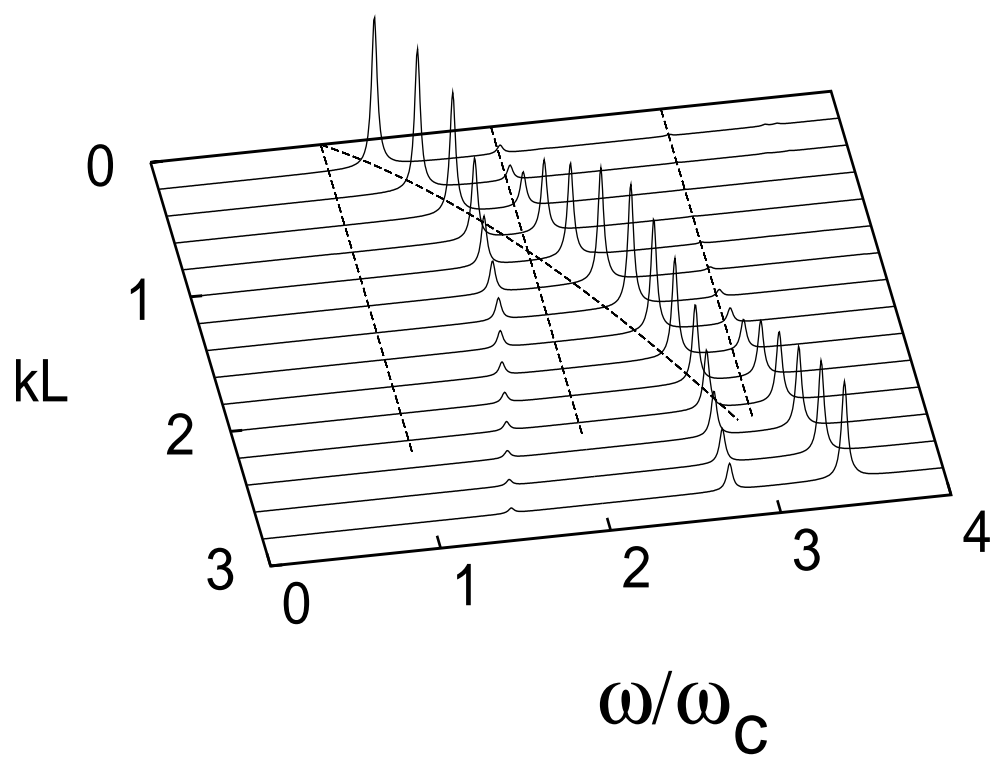
## FIGURES

FIG. 1. The power absorption  $P(k_1, \omega)$  for a homogeneous 2DEG ( $V_0 = 0$ ). The dashed straight lines represent the frequencies of the cyclotron resonances  $\omega = n\omega_c$  and the dashed curve is the dispersion of the magnetoplasmon in first order with respect to  $k_1$ .  $L = 200$  nm,  $pq = 1$ ,  $\nu = 1$ ,  $m^* = 0.067m_0$ ,  $T = 1$  K,  $\kappa = 12.4$ , and  $\hbar\omega_c = 0.178$  meV.

FIG. 2. (a) The power absorption  $P(k_1, \omega)$  (in arbitrary units) for a modulated 2DEG ( $V_0 = 4$  meV). The solid curve in the  $(k_1, \omega)$ -plane represents the dispersion of the magnetoplasmon of a homogeneous 2DEG in first order with respect to  $k_1$ . (b) The low frequency region repeated from (a). The left peak decreases with increasing wave vector,  $k_1$ . (c) The dispersion of the two lowest Landau bands in the quasi-Brillouin zone along several values of  $\theta_2$  projected on the  $\theta_1$  axis (each band is split into three subbands). The chemical potential is indicated by a solid horizontal line.  $pq = 3$ ,  $L = 50$  nm,  $\nu = 1/2$ , and  $\hbar\omega_c = 8.57$  meV.

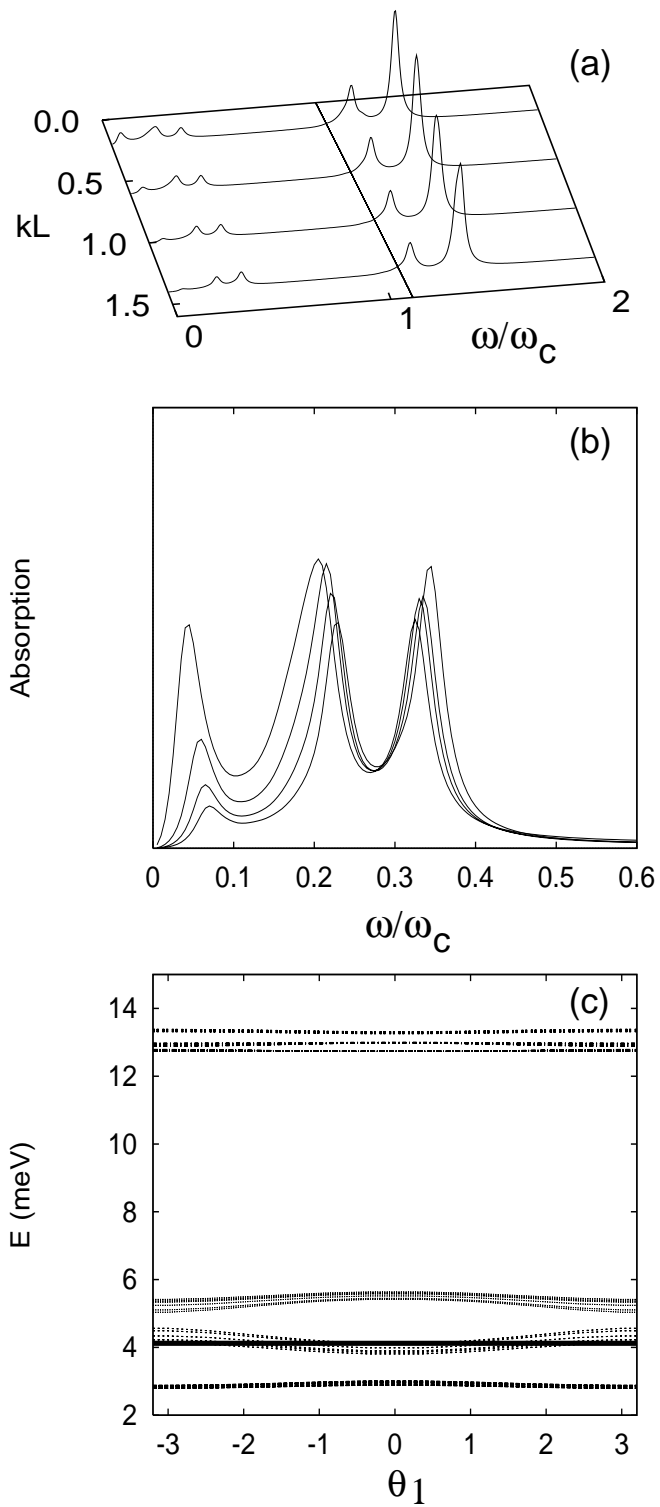
FIG. 3. (a) The power absorption  $P(k_1, \omega)$  for a modulated 2DEG ( $V_0 = 4$  meV). The solid curve in the  $(k_1, \omega)$ -plane represents the dispersion of the magnetoplasmon in a homogeneous 2DEG in the first order with respect to  $k_1$ . (b) The dispersion of the two lowest Landau bands in the quasi-Brillouin zone along several values of  $\theta_2$  projected on the  $\theta_1$  axis (each band is split into three subbands). The chemical potential is indicated by a solid horizontal line.  $pq = 3$ ,  $L = 50$  nm,  $\nu = 5/6$ , and  $\hbar\omega_c = 8.57$  meV.

FIG. 4. The power absorption  $P(k_1, \omega)$  for a modulated 2DEG in two cases; (solid)  $pq = 2$ ,  $L = 100$  nm,  $\nu = 1/2$ ,  $\hbar\omega_c = 1.43$  meV, and  $V_0 = 0.4$  meV, and (dashed)  $pq = 4$ ,  $L = 50$  nm,  $\nu = 7/8$ ,  $\hbar\omega_c = 11.4$  meV, and  $V_0 = 3$  meV.  $k_1 L = 0.6$ , and  $T = 1$  K in both cases.

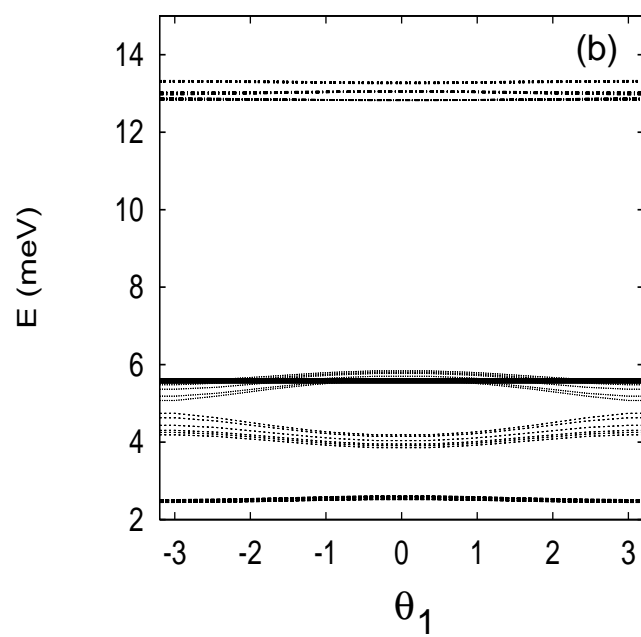
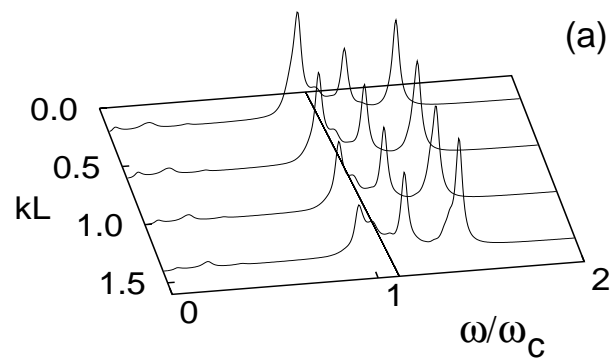


Gudmundsson, Fig. 1

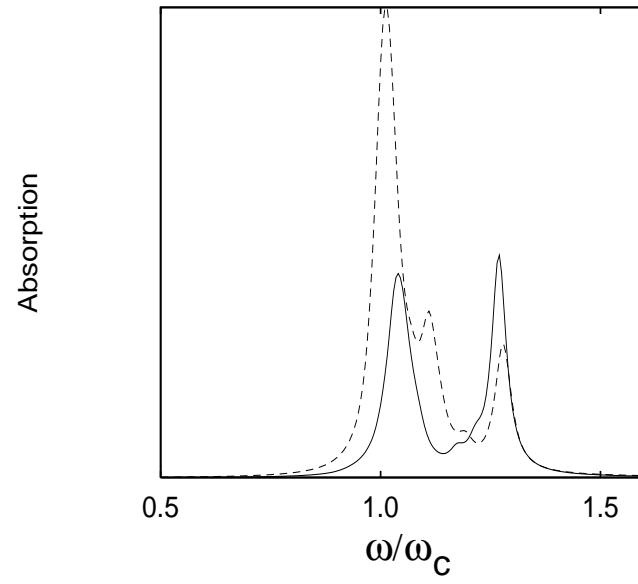




Gudmundsson, Fig. 2



Gudmundsson, Fig. 3



Gudmundsson, Fig. 4